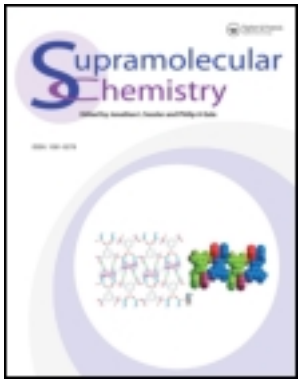

Supramolecular Chemistry
Publication details, including instructions for authors and subscription information:
http://www.tandfonline.com/loi/gsch20

Reactivity of carbonyl and phosphoryl groups at calixarenes

Roberta Cacciapaglia[a], Stefano Di Stefano[a], Luigi Mandolini[a] & Riccardo Salvio[a]
[a] Dipartimento di Chimica and IMC-CNR Sezione Meccanismi di Reazione, Università La Sapienza, P.le Aldo Moro 5, 00185, Roma, Italy
Published online: 25 Aug 2013.

To cite this article: Roberta Cacciapaglia, Stefano Di Stefano, Luigi Mandolini & Riccardo Salvio (2013) Reactivity of carbonyl and phosphoryl groups at calixarenes, Supramolecular Chemistry, 25:9-11, 537-554, DOI: 10.1080/10610278.2013.824578

To link to this article: http://dx.doi.org/10.1080/10610278.2013.824578

Supramolecular Chemistry, 2013
Vol. 25, Nos. 9–11, 537–554, http://dx.doi.org/10.1080/10610278.2013.824578

Taylor & Francis
Taylor & Francis Group

Reactivity of carbonyl and phosphoryl groups at calixarenes

Roberta Cacciapaglia*, Stefano Di Stefano, Luigi Mandolini and Riccardo Salvio

Dipartimento di Chimica and IMC-CNR Sezione Meccanismi di Reazione, Università La Sapienza, P.le Aldo Moro 5, 00185 Roma, Italy

(*Received 23 June 2013; final version received 9 July 2013*)

Examples of reactivity of carbonyl and phosphoryl compounds controlled by calixarenes are illustrated in this review article. The molecular framework of calixarenes has been widely used as a versatile molecular platform for the dynamic arrangement of one or more structural units working as recognition and/or catalytic sites, in many cases with considerable levels of cooperation. The calixarene cavity itself has also been involved as a recognition unit for inclusion of the substrate or of part-structures of the substrate. Unique reactivity patterns of carbonyl or phosphoryl functional groups organised at the upper or lower rim of calixarenes will also be illustrated.

Keywords: catalysis; enzyme mimics; host–guest; guanidinium; metal ion

The ability of calixarenes (*1*, *2*) to form host–guest complexes with the possible involvement of their molecular cavity in the recognition process, coupled with the ease of selective derivatisation of either rim with a variety of ligand moieties and functional groups in diverse mutual geometrical arrangements, has contributed to the broad success of this class of macrocycles as multifunctional catalysts and enzyme mimics. Furthermore, functional groups properly preorganised at the calixarene molecular platform have also shown in a number of cases unique reactivity features, originating from intramolecularity.

Access to a fine control of conformational properties, together with retention of a residual degree of flexibility in the molecular scaffold suitably preorganised in a fixed *cone* conformation, is a key feature of these reaction systems. Reinhoudt et al. (*3*) introduced the notion of 'dynamic preorganisation' to describe the capability of calixarenes to guarantee a good compromise between a well preorganised set of recognition and/or catalytic groups and a residual flexibility. These features greatly help in the dynamic fit of the catalyst to the bound substrate throughout its transformation into the transition state.

In this review article, we focus on reactivity of carbonyl and phosphoryl groups promoted by calixarenes or involving calixarenes. Results obtained with cavitands or, in general, with resorcinarene-based systems, will not be mentioned here.

1. A calixarene-based nucleophilic catalyst with transacylase activity

A fairly efficient nucleophile catalyst with transacylase activity (**1**-Ba; ***cat***) was developed in the early 1990s by Mandolini and Ungaro and co-workers (*4*). Previous investigations had shown that alkaline earth metal ions are efficient promoters of acyl transfer reactions from esters to anionic nucleophiles, and that the observed rate enhancements are larger when the alkaline earth metal ions are complexed by crown ethers. This is particularly so when the ester function is covalently linked to a proximal metal ion binding site (*5*). The barium complex **1**-Ba, generated *in situ* from an equimolar mixture of *p-tert*-butylcalix[4]arene-crown-5 $\mathbf{1}(H^+)_2$ and barium salt under slightly basic conditions [3:1, diisopropylethylamine:perchlorate salt buffer in MeCN:MeOH (9:1, v/v), 25°C], was found to act as a turnover catalyst in the methanolysis of a series of aryl acetates (Figure 1), according to a double displacement (*ping-pong*) mechanism (Scheme 1). The barium ion acts as a built-in electrophilic catalyst. It favours nucleophile addition to carbonyl both in the acyl transfer from the ester substrate (ArOAc) to ***cat*** in the acylation step, and in its subsequent transfer from the acylated catalyst (***catAc***) to the external nucleophile (solvent) in the deacylation step, thus restoring the active form of the catalyst.

The key feature underlying the efficiency of the catalytic mechanism is the preorganisation on the same calix[4]arene platform of the electrophile catalyst (*E*, the Ba^{2+} ion) in close proximity of the nucleophile (*N*, the phenoxide ion) in the acylation step, or in close proximity of the substrate *S* (the acetyl function of ***catAc***) in the deacylation step (Scheme 1). The slow liberation of *p*-nitrophenol due to background methanolysis (Figure 1) is unaffected by the addition of $\mathbf{1}(H^+)_2$ alone. Biphasic kinetics obtained in the presence of **1**-Ba are typical of proteolytic enzymes (chymotrypsin) and are consistent with a double displacement mechanism in which fast

*Corresponding author. Email: roberta.Cacciapaglia@uniroma1.it

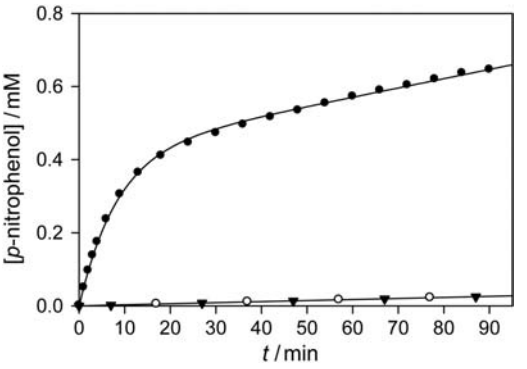

Figure 1. Liberation of *p*-nitrophenol in the methanolysis of 3.0 mM *p*-nitrophenyl acetate. The initial burst of *p*-nitrophenol is followed by a steady-state phase. (▼) Background reaction in the presence of buffer alone; (○) buffer plus 0.46 mM **1** $(H^+)_2$; (●) buffer plus 0.46 mM **1**$(H^+)_2$ and 0.46 mM $BaBr_2$, data from Ref. (*4*).

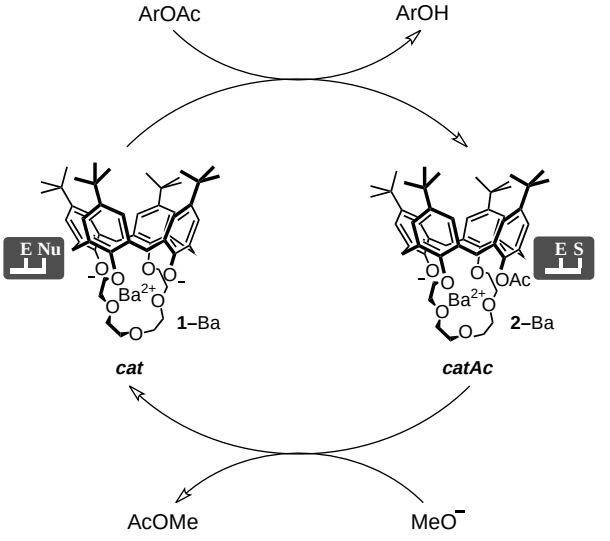

Scheme 1. Turnover nucleophilic catalysis of **1**-Ba in the methanolysis of aryl acetates.

acylation of ***cat*** is followed by slower deacylation of the acylated form ***catAc***. At variance with natural enzymes, no binding site is present in the calixarene catalyst **1**-Ba for substrate recognition. The initial burst of *p*-nitrophenol release is followed by a slower linear phase, corresponding to an exact balance between formation and destruction of the acylated intermediate, whose concentration reaches a constant plateau value. Consistent results were obtained by high-performance liquid chromatography monitoring of the accumulation of ***catAc***.

The crucial importance of a certain degree of flexibility in the calix[4]arene platform is shown by the lack of any catalytic activity of the barium salts of rigidified structures **3** and **4** (*6*).

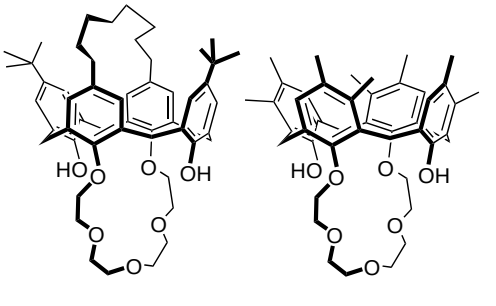

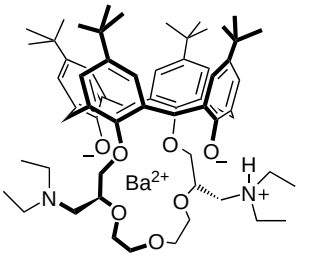

In the methanolysis of a series of aryl acetates (XC_6H_4OAc, X = *p*-NO_2, *m*-NO_2, *p*-Cl, H) catalysed by **1**-Ba, a gradual changeover from rate-determining deacetylation (with the most reactive *p*-nitrophenyl acetate) to rate-determining acetylation (with the least reactive phenyl acetate) was observed (*7*). In the aim at enhancing the slow acetylation step, catalyst **5**-Ba was designed. The protonated amino group in **5**-Ba indeed assisted as a general acid the slow decomposition of the tetrahedral intermediate of the rate-determining acetylation step, but the catalytic efficiency was hampered by the steric hindrance of the bulky diethylaminomethyl side-arm.

2. Calixarene-based artificial esterases

Providing the calixarene-based catalysts with suitable recognition sites for substrate binding was a further decisive step towards the development of calixarene-based enzyme mimics, showing substrate-selectivity and Michaelis–Menten saturation kinetics.

2.1 Dinuclear metalloesterases

Many hydrolytic enzymes possess two or three metal ions in their active site (*8*). Consequently, there has been a wide interest in the biomimetic hydrolytic activity of dinuclear and trinuclear metal complexes (*9*). In the ambit of these investigations, calixarenes have been extensively used as suitable spacers connecting metal complexing units. The use of the upper rim of calix[4]arenes blocked in the *cone* conformation in the development of biomimetic catalysts was successfully pioneered by the group of

Reinhoudt and co-workers (*3*). Further investigations from joint efforts of Reinhoudt's group in Enschede, Ungaro's group in Parma and Mandolini's group in Roma have been aimed at widening the scope of the calix[4]arene scaffold in the construction of di- and trinuclear catalysts capable of esterase activity and in the development of water-soluble artificial hydrolases.

2.1.1 *Artificial esterases: barium(II) complexes*

Calix[4]arene-based bimetallic complexes **12**-Ba_2 and **13**-Ba_2 are turnover catalysts of the basic ethanolysis of esters **6**–**9** functionalised with a distal carboxylate anchoring group, according to the mechanism depicted in Scheme 2 (*10*). The barium ion is the core both of the recognition and catalytic site of these artificial esterases.

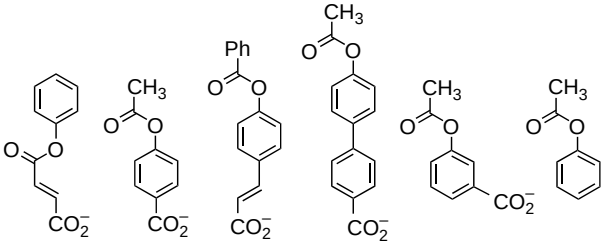

6 **7** **8** **9** **10** **11**

The high affinity of carboxylate for the complexed barium ion ensures efficient binding of the ester substrate to the metal catalyst. The function of the anchoring step is manifold: it selects the substrate, provides electronic activation to the ester undergoing nucleophilic attack by conversion of a moderately electron-releasing (rate-retarding) substituent into an electron-withdrawing (rate-enhancing) substituent and, more importantly, transforms an otherwise intermolecular ethoxide delivery to the ester carbonyl into an intramolecular (intracomplex) ethoxide delivery. Rate enhancements ranged from one to more than four orders of magnitude, with a marked dependence on the individual substrate–catalyst combination.

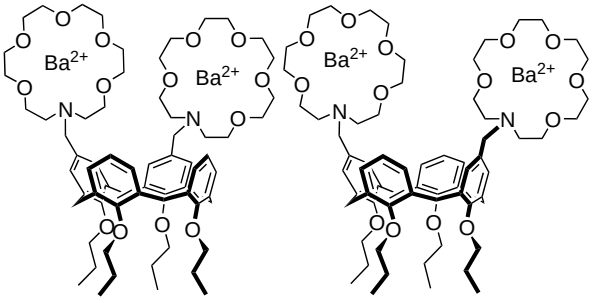

12-Ba_2 **13**-Ba_2

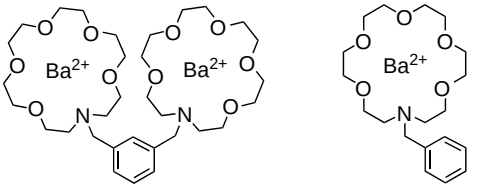

14-Ba_2 **15**-Ba

The catalysts were tested under reaction conditions where no less than 90% of the ester is bound in the productive (Michaelis) complex **II** (Scheme 2), while the concentration of the unproductive 2:1 complex **III** is negligibly low [EtOH, 25°C, 0.025 mM substrate, 1 mM $EtONMe_4$, 0.2 mM monotopic or 0.1 mM ditopic ligand, 0.2 mM $Ba(SCN)_2$]. The marked superiority shown by dinuclear catalysis over the mononuclear counterpart confirms that the

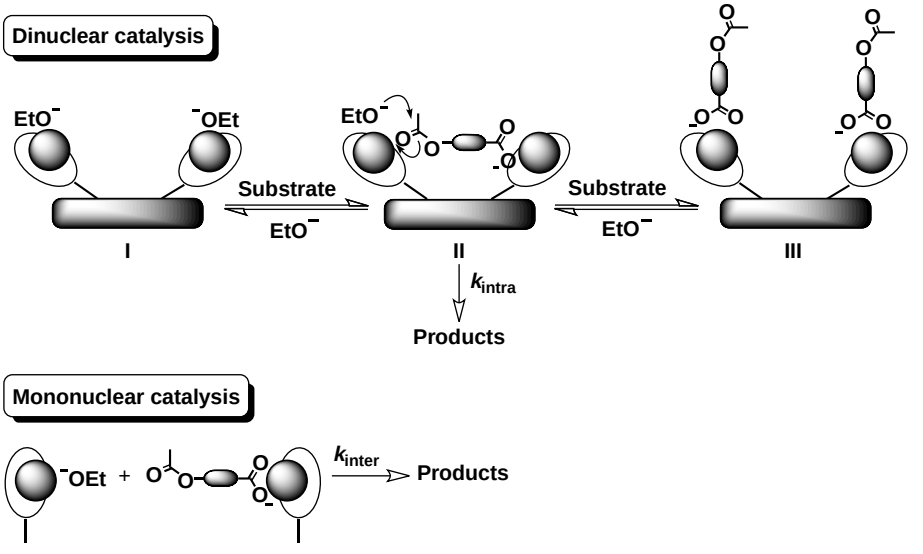

Scheme 2. (a) Mechanism of ester ethanolysis catalysed by dinuclear barium complexes, showing productive (**II**) and non-productive (**I** and **III**) species and (b) the corresponding intermolecular model reaction based on mononuclear complexes.

two metal ions work together in a cooperative fashion, in accordance with the bifunctional catalytic mechanism reported in Scheme 2. In the basic ethanolysis of **7**, for example, the rate observed in the presence of 0.1 mM **12**-Ba_2 is notably more than three orders of magnitude higher than the rate observed in the presence of 0.2 mM mononuclear control **15**-Ba. In order to get effective catalysis, the target substrate and the catalyst must form a well-matched pair in terms of size and geometrical features. Accordingly, the choice of the scaffold on which the metal ion ligating units are implanted is crucial for the obtainment of a high level of cooperation.

Catalytic performances of regioisomeric **12**-Ba_2 and **13**-Ba_2 and those of the complex **14**-Ba_2 featuring a *m*-xylylene spacer were compared in terms of effective molarities (EMs) (*11, 12*). The EM notion, defined by the ratio k_{intra}/k_{inter} (Scheme 2), provides a convenient measure of the advantage coming from intramolecularity in the process catalysed by the bifunctional catalyst. The EM value is independent of the chemical activation provided by the catalytic groups, and solely depends on the way the catalyst template organises reactants in a geometry suitable for the occurrence of the reaction. At variance with the catalytic rate enhancement and the advantage of dinuclear over mononuclear catalyst, the EM value is independent of reactant concentrations, its numerical value being solely determined by the choice of molarity as concentration unit. Plots of EM versus the carboxylate–carbonyl distances $C_{carbonyl}-C_{carboxyl}$ in the ester substrates, taken as a gross estimate of their size (Figure 2), show that a good match of ester size to metal-to-metal distance is an important prerequisite for catalysis. In this plot, the catalytic performance of calixarene versus *m*-xylylene spacer is evaluated. The dinuclear catalyst **12**-Ba_2, in which the azacrown units are linked to 1,2-vicinal positions in the calix[4]arene scaffold, is not only far superior to its 1,3-distal regioisomer **13**-Ba_2 in all cases, but it is also superior to the *m*-xylylene derivative **14**-Ba_2 (*13*) in the reactions of esters **6**–**8**.

The efficiency of the intramolecular (intracomplex) process involving the bifunctional catalyst and reactants is strongly influenced by the number of skeletal single bonds involved in the generation of the pseudo-cyclic array at the transition state, because a part of the torsional entropy is lost. A general extrathermodynamic treatment (*11b*) relates the entropy loss upon cyclisation, and hence the entropic component of the EM (EM_S), to the number of rotatable bonds in the open chain reactant undergoing cyclisation, and provides the corresponding set of predicted EM_S values. Under the assumption that the carboxylate–metal–(crown ether) and ethoxide–metal–(crown ether) moieties can be assimilated to pseudo-single bonds and that the torsional entropy associated with such pseudo-bonds is comparable with that of a covalent bond, in the productive complex involved in the ethanolysis of esters **7** and **8** catalysed by **12**-Ba_2 there are

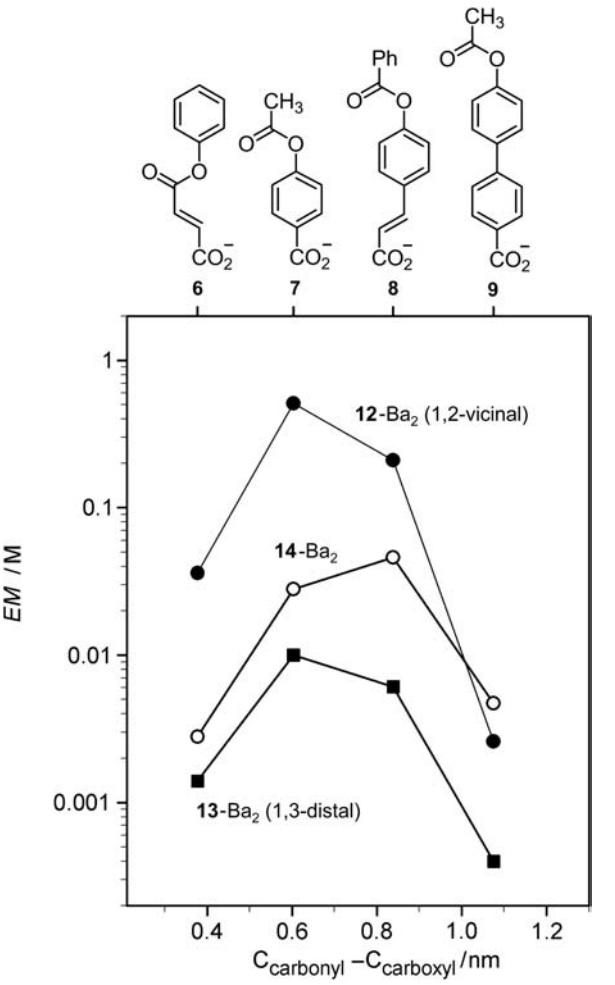

Figure 2. Calixarene versus *m*-xylylene spacer. Basic ethanolysis of esters **6–9** catalysed by the barium complexes of ligands **12**–**14** (for ester **8**, the quoted $C_{carbonyl}-C_{carboxyl}$ distance is an average value). Data from Refs. (*10, 13*).

9 and 10 rotatable bonds, respectively, translating into predicted EM_S values of 0.67 and 0.47 M, in the given order. These values compare fairly well with the experimental EM values 0.51 and 0.21 M, respectively, for the ethanolysis of esters **7** and **8** catalysed by **12**-Ba_2. A reasonably good match between transition state and bimetallic catalyst is thus apparent in these systems. With the same substrates, the catalytic performances of the 1,3-distal calixarene spacer in **13**-Ba_2 and those of the *m*-xylylene spacer in **14**-Ba_2 are definitely lower, pointing to the existence of severe mismatch between transition state and bimetallic catalyst.

2.1.2 *Artificial esterases: zinc(II) complexes*

Regioisomeric dinuclear complexes **16**-Zn_2 and **17**-Zn_2 are shape- and size-selective turnover catalysts of the methanolysis of esters **7**–**10** provided with a carboxylate anchoring group [MeOH, pH 10.4 (*N*,*N*-diisopropyl-*N*-(2-methox-

yethyl)amine buffer), 25°C] (*14, 15*). In marked contrast to the behaviour of phenyl acetate **11**, the reactions of the esters **7**–**10** functionalised with a distal carboxylate are catalysed by dinuclear complexes **16**-Zn_2 and **17**-Zn_2 much more efficiently than by the mononuclear zinc(II) complex with 2,6-*bis*[(dimethylamino)methyl]pyridine (BAMP). The superiority of the bimetallic catalyst over the monometallic model is larger than two orders of magnitude in the most favourable cases. The picture is consistent with a bifunctional catalytic mechanism in which the two complexed metal ions work in a cooperative fashion (Figure 3). One of the metal ions serves as a docking site for carboxylate and the other delivers intramolecularly an activated methoxide to the ester function of the complexed substrate. Rate enhancements larger than four orders of magnitude were observed in the reaction of **10** catalysed by the 1,2-vicinal complex **16**-Zn_2.

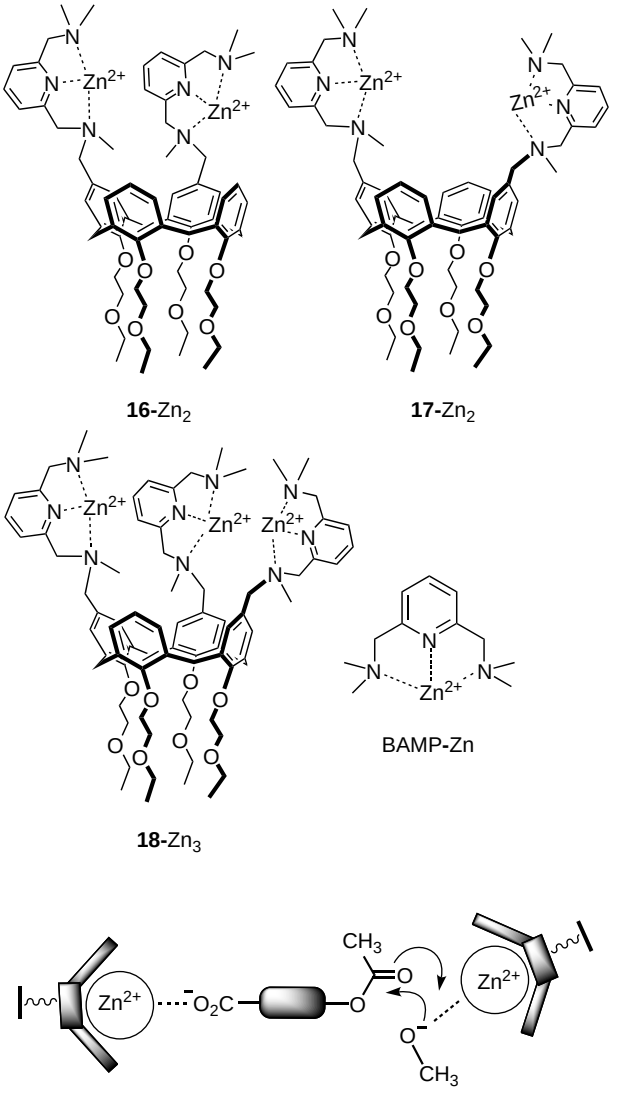

Figure 3. Bimetallic catalytic mechanism in the basic methanolysis of esters functionalised with a distal carboxylate anchoring group.

The marked superiority of the 1,2-vicinal complex **16**-Zn_2 over its distal regioisomer **17**-Zn_2 closely parallels that observed in the basic ethanolysis catalysed by dinuclear complexes **12**-Ba_2 and **13**-Ba_2. The results obtained in the basic methanolysis of esters catalysed by the zinc(II) complexes of calix[4]arenes **37** and **38** decorated with 1,5,9-triazacyclododecane ([12]aneN_3) ligands (see also Section 3.2.2 for the use of these complexes as artificial phosphodiesterases) fully confirm the superiority of 1,2-vicinal bimetallic catalysts over their 1,3-distal regioisomers (*16*). The order of catalytic efficiency 1,2-vicinal >> 1,3-distal appears to be a substrate-independent feature of upper rim calix[4]arene-based bimetallic catalysts for the cleavage of carboxylate-functionalised esters, which is unaffected by the nature of the metal ion and of the corresponding ligating unit.

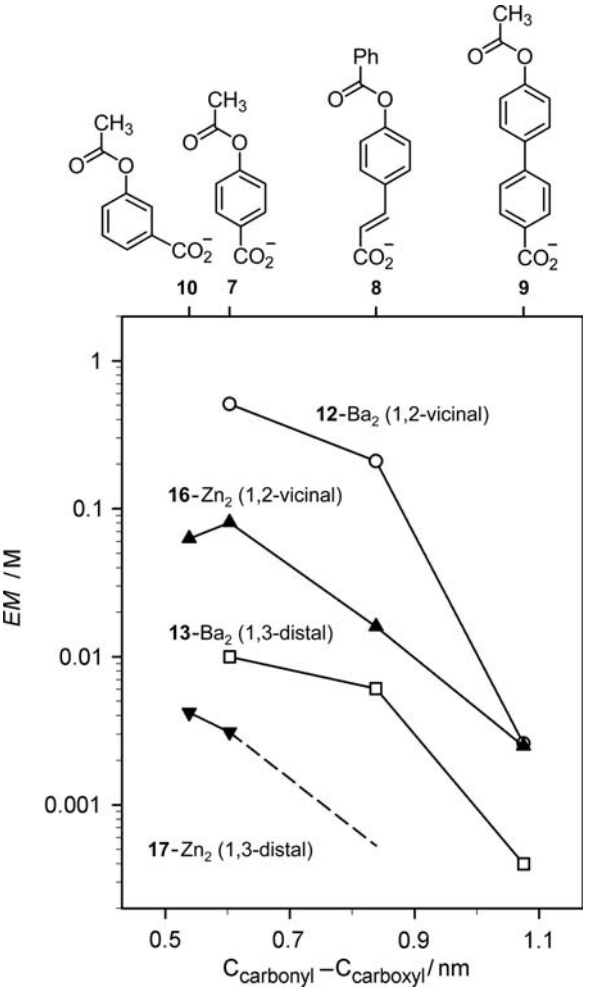

Figure 4. Calix[4]arene-zinc(II) versus calix[4]arene-barium (II) catalysts. Basic alcoholysis of esters catalysed by barium(II) complexes of ligands **12** and **13** and zinc(II) complexes of ligands **16** and **17** (for ester **8**, the quoted $C_{carbonyl}-C_{carboxyl}$ distance is an average value). Data from Refs. (*10, 15*).

A meaningful comparison between the catalytic performance of barium(II) complexes **12**-Ba_2 and **13**-Ba_2 in the basic ethanolysis of carboxylate-functionalised esters, with that of zinc(II) complexes **16**-Zn_2 and **17**-Zn_2 in the basic methanolysis of the same substrates, is allowed in terms of effective molarities. EM data are plotted in Figure 4 together with available data for the basic ethanolysis catalysed by dinuclear complexes **12**-Ba_2 and **13**-Ba_2. A definite superiority of **12**-Ba_2 and **13**-Ba_2 over the structurally related **16**-Zn_2 and **17**-Zn_2 emerges, indicating a lower adaptability of the zinc(II) complexes to the altered substrates in the transition state, which is consistent with the more stringent requirements of the coordinative interactions of a *d*-block metal ion compared with an *s*-block metal ion.

2.2 *Artificial esterases: trimetallic zinc(II) complexes*

Evidence of unprecedented trimetallic catalysis in ester cleavage was obtained in the investigation of the catalytic activity of calix[4]arene trinuclear complexes **18**-Zn_3 and **39**-Zn_3 in the methanolysis of esters provided with a carboxylate anchoring group (*14, 15*).

The advantage of the trimetallic catalyst **18**-Zn_3 over the 1,2-bimetallic catalyst **16**-Zn_2 in the cleavage of **7** is definitely higher than the calculated statistical advantage (*15*) of the trimetallic complex over its bimetallic analogues. Some evidence of trimetallic catalysis is also obtained in the cleavage of **7** catalysed by **18**-Zn_3 and in the cleavage of **10** catalysed by **39**-Zn_3. Figure 5 illustrates the different functions performed by the three metal ions cooperating in the proposed catalytic mechanism: (i) substrate recognition through binding to carboxylate, (ii) Lewis-acid activation of the ester carbonyl and (iii) nucleophile delivery.

2.3 *Peptidocalix[4]arenes as artificial esterases*

Hioki et al. (*17*) developed a set of peptidocalix[4]arene catalysts (Figure 6) of the hydrolysis of ester **19** (Equation (1)). Promising structures were selected among components of a resin-bound peptidocalix[4]arene library by binding assay with the aniline-labelled transition state analogue **20**.

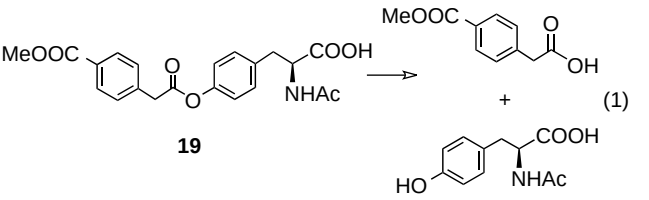

19

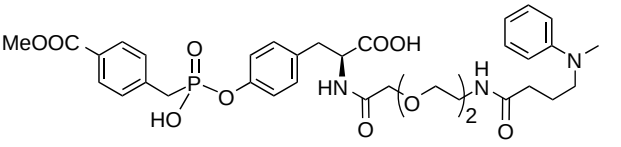

20

From hydrolysis experiments (1.25 mM **19**, 0.2 equivalent candidate catalyst, aqueous phosphate buffer, pH 6.86, at 30°C), peptidocalix[4]arene **21a** turned out to be the most effective catalyst, with a Michaelis constant $K_M = 1.59 \times 10^{-3}$ M and a >50-fold rate enhancement at saturation.

2.4 *Artificial esterases: the involvement of the calixarene cavity as recognition site*

The cavity of calixarenes has been successfully exploited in the design of the recognition site of supramolecular catalysts, for inclusion of the substrate or part-structure of the substrate.

Previously developed *p*-sulphonatocalix[*n*]arenes **22** (*18*) were used by Ueoka and co-workers (*19*) as water-soluble catalysts of the specific acid catalysed methanolysis of *N*-Ac-L-amino acids (Phe, Tyr, Trp, His, Lys and Arg).

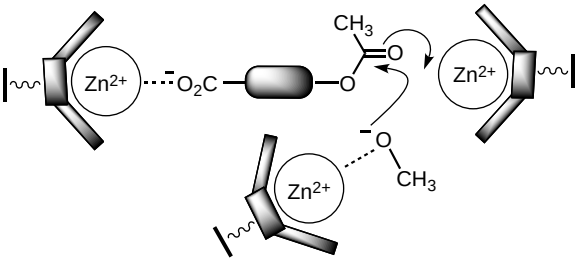

Figure 5. Trimetallic catalytic mechanism in the basic methanolysis of esters functionalised with a distal carboxylate anchoring group.

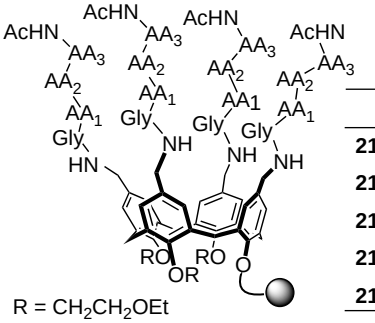

21

	AA_1	AA_2	AA_3
21a	His	Arg	His
21b	Pro	Arg	His
21c	Tyr	Lys	His
21d	Ser	Lys	His
21e	Glu	Glu	Glu

Figure 6. Selected candidate catalysts **21a**–**e** of the hydrolysis of ester **19**.

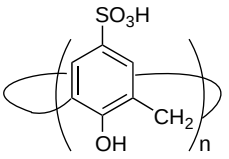

22 (n = 4 , 6 , 8)

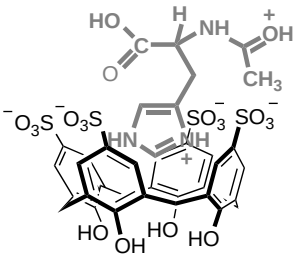

23

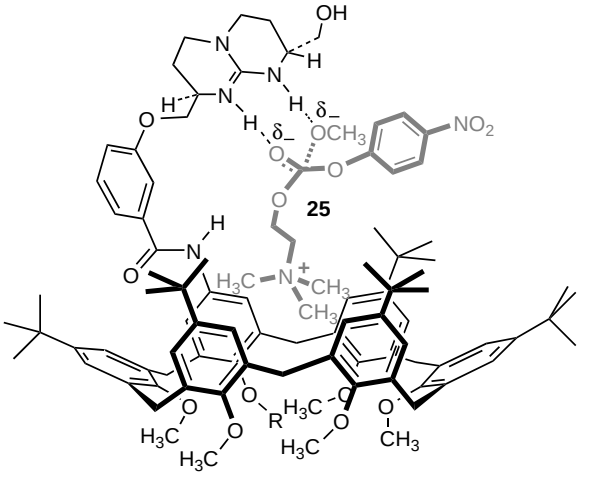

24a, R = H

24b, R = H_2C 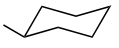

Rates of methanolysis observed in the presence of the calix[*n*]arene catalysts **22**, normalised per sulphonic group, are compared with rates obtained in the presence of non-cyclic analogue *p*-hydroxybenzenesulphonic acid. In the methanolysis of basic amino acid derivatives (His, Lys and Arg), rate enhancements observed in the presence of *p*-sulphonatocalix[*n*]arenes **22** are from 12- to 86-fold higher than those observed in the presence of the non-cyclic control. On the other hand, in the reaction of neutral *N*-Ac-L-amino acids (Phe, Tyr and Trp), virtually the same rate enhancements are obtained in the presence of cyclic and non-cyclic catalysts. Michaelis–Menten kinetics and ^{1}H NMR spectral evidence pointed to the intermediacy of inclusion complexes of *p*-sulphonatocalix[*n*]arenes **22** with the protonated form of basic amino acid derivatives, as shown in **23** for the His-**22** ($n = 4$) combination.

The calix[6]arene cavity plays a key role in substrate recognition in the artificial acethylcholinesterase **24** developed by de Mendoza et al. (*20*). Anionic phosphodiesters have been widely used as transition state analogues for the basic hydrolysis of esters. Accordingly, ditopic receptors **24** were designed and synthesised (*20a*) as mimics of the phosphocholine-binding site of McPC603 antibody.

Effective recognition of dioctanoyl-L-α-phosphatidylcholine by **24** occurs ($K = 73{,}000\,M^{-1}$ for **24a** and $95{,}000\,M^{-1}$ for **24b** in chloroform, 25°C) as a result of combined interactions of the choline trimethylammonium head with the calix[6]arene subunit through cation–π interactions and of the anionic phosphodiester group to the guanidinium subunit through cation–anion interactions reinforced by hydrogen bonding. The methanolysis of *p*-nitrophenylcholine carbonate (PNPCC) (Equation (2)) is effectively catalysed with turnover by **24** ($CHCl_3$/MeOH 99:1; diisopropylethylamine–perchlorate salt buffer, 25°C) (*20b*).

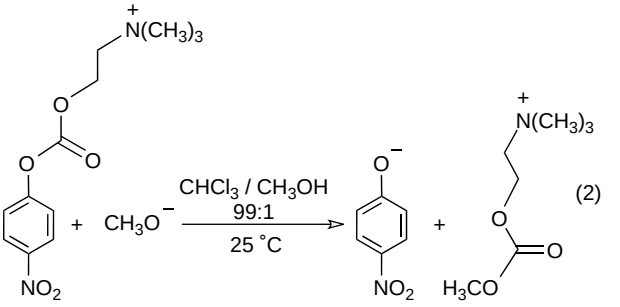

(2)

A rate enhancement of 76-fold over background is recorded in the presence of 1 mM **24a**, and one of 149-fold in the presence of 1 mM **24b**. Definitely lower rate enhancements are obtained in the presence of equimolar mixtures of the disconnected subunits, showing that the two subunits in **24** bind to the transition state **25** with a significant degree of synergism. Kinetic analysis predicts maximum rate accelerations at saturation of 600 and 1000 for **24a** and **24b**, respectively.

3. Calixarene-based artificial phosphodiesterases

3.1 Guanidinocalix[4]arenes as artificial phosphodiesterases and adenosine triphosphatases (ATPases)

The guanidinium unit plays a key role in the activity of natural enzymes such as staphylococcal nuclease (*21*) and has been extensively used as an activating and/or anchoring group in the design of hydrolytic catalysts (*22*). Artificial phosphodiesterases **26**–**29** (*23*) were designed by introducing two to four guanidinium units at the upper rim of a *cone* calix[4]arene scaffold.

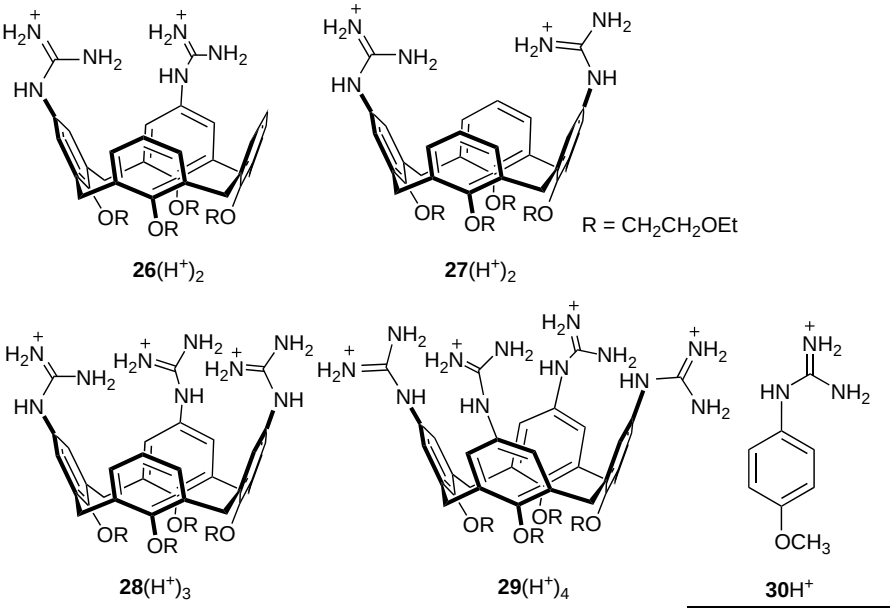

The catalytic activity of guanidinocalix[4]arenes **26**–**29** was tested in the transesterification (Equation (3)) of the RNA model compound 2-hydroxypropyl *p*-nitrophenyl phosphate (HPNP) in 80% dimethyl sulfoxide (DMSO), 25°C, at pH 9–12, corresponding to neutral to moderately basic solutions ($pK_w = 18.4$ in 80% DMSO, at 25°C) (*23*).

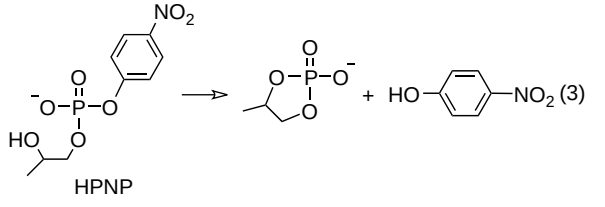

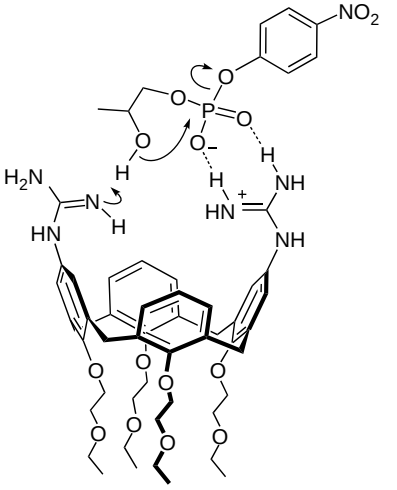

Figure 7. Bifunctional general-acid/general-base catalysis of **27**H^+ in the transesterification of HPNP.

Combination of potentiometric acidity measurements with the pH-dependence of catalytic rates showed that a necessary requisite for effective catalysis is the presence, on the same molecular framework, of the guanidine–guanidinium pair, the neutral guanidine acting as a general base and a protonated guanidine acting as an electrophilic activator (Figure 7). The most effective catalyst is the 1,3-distal derivative **27**H^+, slightly more efficient than the 1,2-vicinal regioisomer **26**H^+. No evidence of trifunctional catalysis was obtained on the other hand with **28**, the additional guanidinium (guanidine) group acting as a more or less innocent spectator. The mono-, di- and triprotonated forms of the tetrasubstituted calix[4]arene **29** are slightly less effective than the corresponding di- and triguanidinocalix[4]arene derivatives, most probably on account of steric interferences with HPNP caused by overcrowding.

A high degree of synergism originates from preorganisation of the components of the guanidine–guanidinium catalytic dyad at the upper rim of a *cone*-calix[4]arene. At millimolar catalyst concentrations, the transesterification of HPNP catalysed by **26**H^+ or **27**H^+ is indeed three orders of magnitude faster than that catalysed by a 1:1 mixture of monofunctional counterparts **30** and **30**H^+.

The triprotonated form **29**$(H^+)_3$ of *cone*-tetraguanidinocalix[4]arene proved to be a highly efficient and selective turnover catalyst of ATP hydrolysis (Equation (4)) (*24*), a process of well-known biochemical relevance. In the reaction medium (80% DMSO, 0.1 M Me_4NClO_4, 80°C), the concentration of **29**$(H^+)_3$ is at a maximum at pH 9.8.

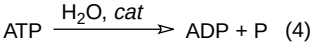

At this pH value, the cleavage of 10 mM ATP carried out in the presence of 0.2 mM guanidinocalix[4]arene **29** is at

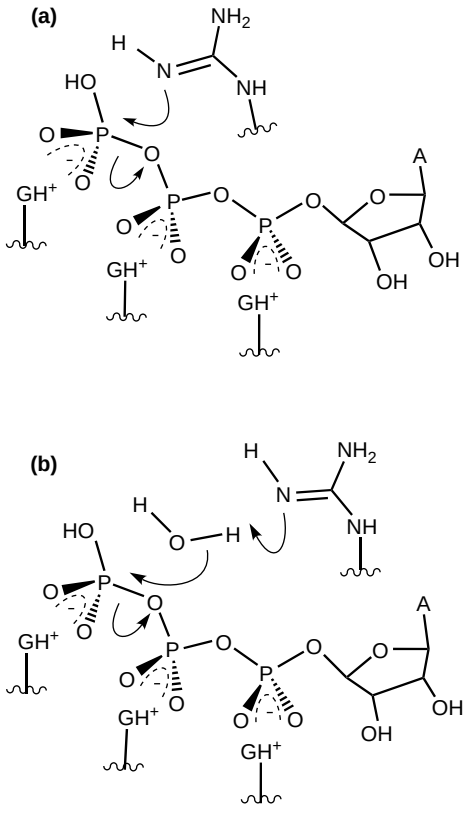

Figure 8. Catalytic cleavage of ATP promoted by **29**$(H^+)_3$. Alternative modes of action of neutral guanidine: (a) nucleophilic catalysis and (b) general-base catalysis.

least three orders of magnitude faster than the reaction carried out in the absence of catalyst. In the active species **29**$(H^+)_3$, the combined action of a neutral guanidine and that of three protonated guanidinium units induces a catalytic activity rivalling that of (*24*) N_6O_2 and related macrocyclic polyamines developed by Lehn and co-workers (*25*). The three protonated guanidinium groups in **29**$(H^+)_3$ bind and activate the substrate, while the neutral guanidine, in analogy with the catalytic mechanism reported in the literature for ATP hydrolysis in the presence of extensively protonated macrocyclic polyamines (*25*), most likely acts as a nucleophilic catalyst, yielding adenosine diphosphate (ADP) and a phosphoramidate intermediate (Figure 8). The latter does not accumulate under the conditions of the experiment, undergoes fast hydrolysis and regenerates the active form of the catalyst.

The observed kinetic data are consistent with a reaction mechanism involving fast and reversible 1:1 association between ATP and catalyst, followed by slow decomposition of the complex into products and free catalyst (Scheme 3; $K = 2.4 \times 10^{-2}\,M^{-1}$ and $k_{cat} = 1.5 \times 10^{-2}\,s^{-1}$).

ADP and P bind to the catalyst to a negligible extent and, consequently, no product inhibition nor appreciable

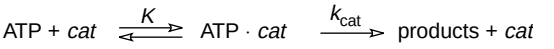

Scheme 3. Catalytic mechanism of ATP hydrolysis.

production of adenosine monophosphate is observed over the entire reaction course.

3.2 *Artificial metallonucleases*

3.2.1 *Zinc(II) and copper(II) complexes of cone-calix[4]arenes as artificial nucleases*

A series of efficient metalloenzyme mimics with phosphodiesterase activity were developed in the late nineties by Reinhoudt et al. (*26*), pioneering the use of calix[4]arenes as molecular scaffolds for the dynamic preorganisation of multiple catalytic groups. The 1,3-distal bimetallic zinc(II) complex **17**-Zn_2 is a highly efficient turnover catalyst of HPNP transesterification (Equation (3)). A 23,000-fold rate enhancement was observed in the presence of 0.48 mM **17**-Zn_2 (50% MeCN-20 mM aqueous buffer, pH 7, at 25°C) (*26*). The two metal ions efficiently cooperate in **17**-Zn_2 both in the binding and in the catalytic conversion of the substrate (Figure 9). The catalytic activity of calix[4]arene **31**-Zn and that of BAMP–Zn are 50-fold and 300-fold lower, respectively (*27, 28*). The sixfold higher activity of **31**-Zn over BAMP–Zn is ascribed to a favourable role of the hydrophobic cavity of the calix[4]arene moiety. In marked contrast to what was observed in the catalytic cleavage of esters, the 1,2-vicinal complex **16**-Zn_2 is significantly less effective than its 1,3-distal regioisomer **17**-Zn_2 in the cleavage of HPNP (*14*). The short crown ether bridge in **32** inhibits the interconversion between *cone* and flattened/pinched *cone* conformations. Complex **32**-Zn_2 cleaves HPNP eight times less effectively than the flexible **17**-Zn_2

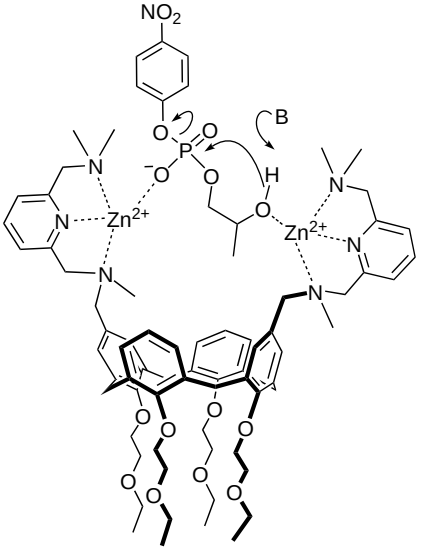

Figure 9. Proposed catalytic mechanism for HPNP cleavage by **17**-Zn_2.

(27), thus confirming the importance of a certain degree of conformational flexibility in the catalyst.

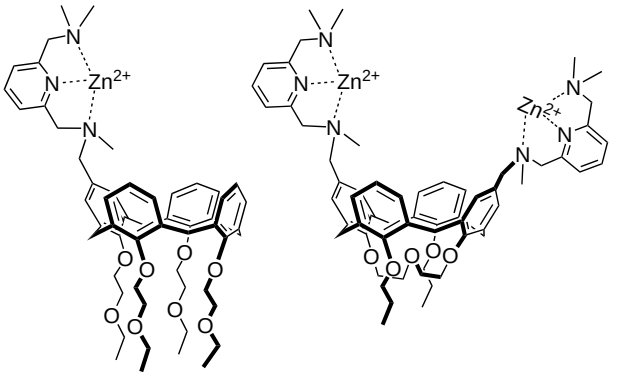

31-Zn **32**-Zn_2

High nuclease activity is shown by the bimetallic copper(II) complex of a calix[4]arene upper rim decorated in 1,3-distal positions with two bidentate ligand moieties derived from *bis*(*N*-methylimidazol-2-yl)methane (28). In 35% EtOH–20 mM aqueous buffer pH 6.2, 25°C, 0.48 mM **33**-Cu_2 induces a rate acceleration of 10,000 in the intramolecular transesterification of HPNP. Also, in this case a strong cooperativity between the metal centres is observed, the mononuclear control **34**-Cu being 22 times less effective.

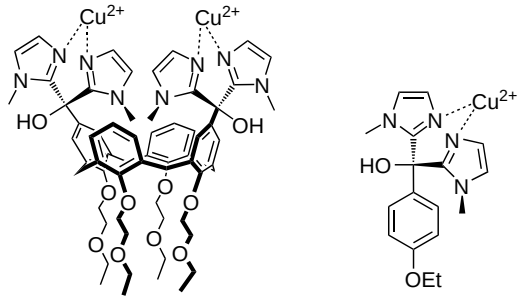

33-Cu_2 **34**-Cu

The copper(II) complex **33**-Cu_2 is not only active in the transesterification of HPNP, but, at variance with **17**-Zn_2 and the much less active **17**-Cu_2 analogue, is also active in the hydrolysis of the DNA model substrate ethyl *p*-nitrophenyl phosphate (EPNP) (28) that reacts via intermolecular nucleophilic attack of a hydroxide ion (Equation (5)). The close proximity of the two metal ions in **33**-Cu_2 allows double Lewis

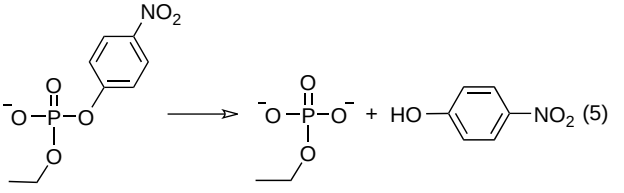

EPNP (5)

acid activation of the phosphoryl group of EPNP and HPNP by the two copper(II) centres. Liberation of *p*-nitrophenol occurs by nucleophilic attack of the metal bound hydroxide ion in the case of EPNP (Figure 10), and of the β-hydroxy group in the case of HPNP. Enhanced catalytic power is obtained upon introduction of a third metal centre (27). The trimetallic complex **18**-Zn_3 shows a threefold increase over **17**-Zn_2 in the specific rate k_{cat} of HPNP transesterification (50% MeCN-20 mM aqueous buffer pH 7, at 25°C). Three zinc(II) ions actually operate in synergy also in the active site of a number of families of metallo-phosphodiesterases such as phospholipase C and nuclease P1, involved in the hydrolytic cleavage of phosphate diester bonds in phosphatidylcholine and phosphatidylinositol and in RNA and DNA, respectively (29). The enhanced catalytic power of **18**-Zn_3 allowed efficient cleavage of diribonucleoside monophosphates (Equation (6)) (30). Rate accelerations in the order of 10^4–10^5 and catalytic turnover are obtained with 0.9 mM **18**-Zn_3 in the cleavage of UpU and GpG (35% EtOH–20 mM HEPES pH 8.0, 50°C), which are cleaved 19- and 160-fold faster than ApA, respectively. Michaelis–Menten saturation profiles obtained in the cleavage of UpU and GpG versus the linear dependency obtained with ApA point to a favourable formation of a productive substrate–catalyst complex with GpG and UpU, and to a negligibly small affinity for ApA. The enhanced binding is ascribed to coordination of a metal centre to a deprotonated amide group in guanosine and uridine.

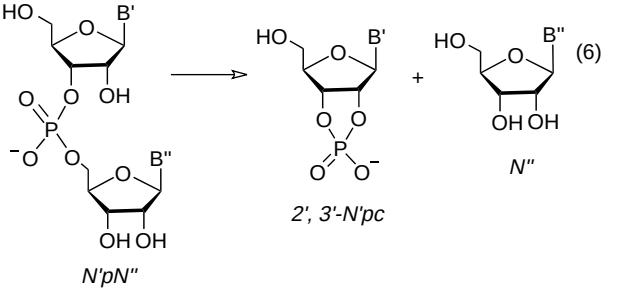

N'pN" *2', 3'-N'pc* *N"* (6)

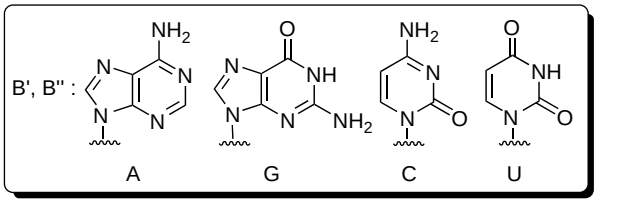

B', B" : A G C U

3.2.2 *Water-soluble artificial metallonucleases*

With the aim of achieving metal catalysts which are soluble enough in water to avoid the use of organic cosolvents, bifunctional and trifunctional calix[4]arenes **37**–**39** decorated with 1,5,9-triazacyclododecane ([12]aneN_3) ligand units were developed (31). The high affinity for zinc(II) and copper(II) ions [log *K* (Zn(II)) = 8.4 (32), and log *K* (Cu(II)) = 12.6 (33), in water, at 25°C] ensures extensive

binding of the metal ion to the [12]aneN$_3$ ligand in water, even at submillimolar concentrations. The relatively low affinity of the BAMP ligand for zinc(II) in water at pH 7.0 (log $K = 3.0$ at 25°C) prevented on the other hand investigation of the RNA nuclease activity of BAMP functionalised catalysts in water, under physiological conditions.

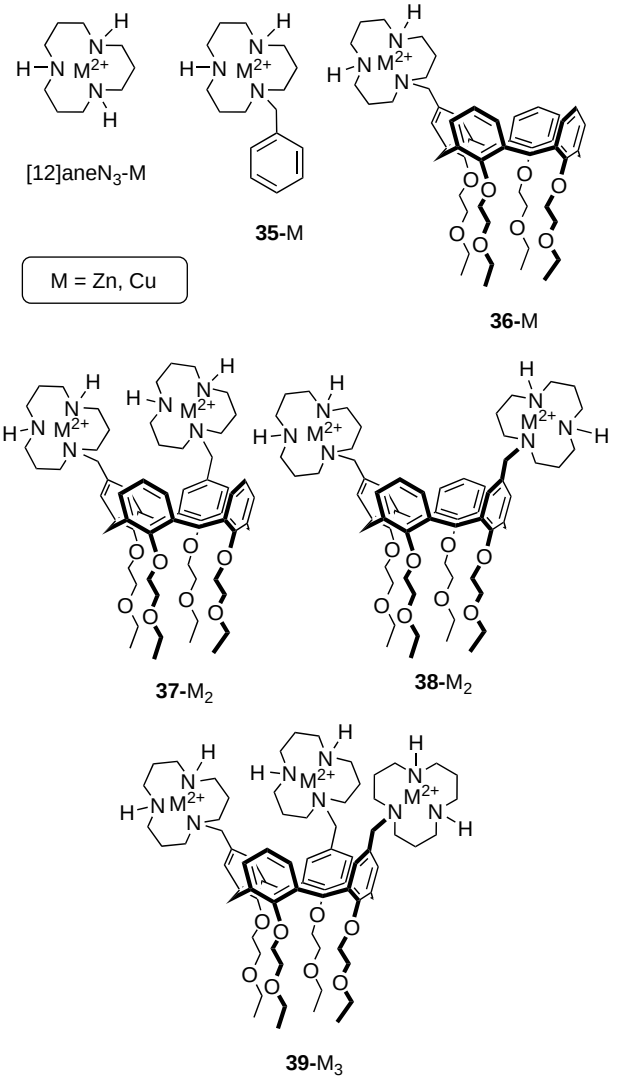

While zinc(II) complexes of ligands **36**–**39** are not soluble in water, the corresponding copper(II) complexes are soluble enough for catalytic studies, the highest solubility being experienced by **39**-Cu$_3$. In the cleavage of HPNP (water, pH 7, 25°C), cooperation between metal centres is significant in the 1,2-vicinal dinuclear complex **37**-Cu$_2$ with a $>10^3$ rate enhancement at 0.2 mM catalyst over the reaction carried out in the presence of buffer alone, and 42-fold and 73-fold accelerations over **35**-Cu and [12]aneN$_3$-Cu, respectively (*31*). In contrast, the catalytic efficiency of 1,3-distal bimetallic regioisomer **38**-Cu$_2$ is about twice as great as that of monometallic

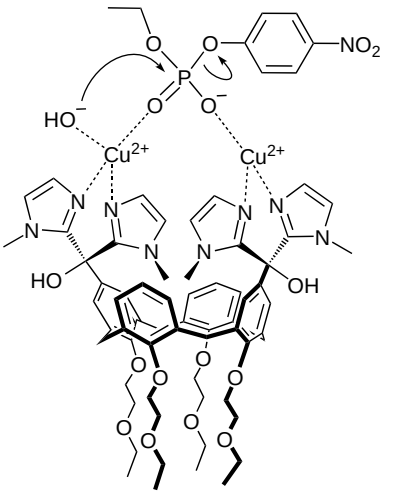

Figure 10. Proposed catalytic mechanism for EPNP cleavage by **33**-Cu$_2$.

35-Cu, with no rate acceleration per metal centre. Trimetallic catalysis is not operative, since the trimetallic complex **39**-Cu$_3$ turns out to behave essentially as a 1,2-vicinal dinuclear catalyst. The Michaelis–Menten profile indicates the reversible formation of a moderately stable HPNP-**37**-Cu$_2$ catalyst complex ($K = 1/K_M = 500\,M^{-1}$). A two-point interaction of the phosphate moiety to the two 1,2-vicinal copper(II) ions with double Lewis-acid activation and the possible involvement of a metal-bound hydroxide as a general base was proposed (Figure 11).

Trimetallic complex **39**-Cu$_3$ cleaves a series of diribonucleoside monophosphates (UpU, UpG, GpU, GpG, ApG, CpG, GpA and CpA) with catalytic rate accelerations in the order of 10^4-fold in most cases (*31*). Rate enhancements rise to 10^5-fold in the cleavage of UpU and UpG and this is believed to be caused by the additional binding site arising from the copper-assisted

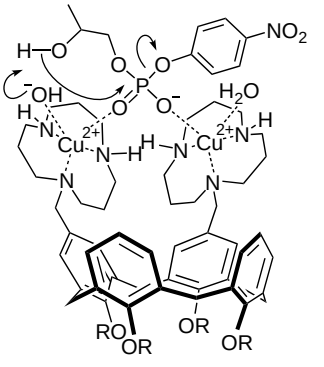

Figure 11. HPNP transesterification in water, catalysed by **37**-Cu$_2$. Proposed mode of substrate binding and activation.

deprotonation of the uracil moiety at the 5′-terminus. Quite unexpectedly, CpA is not cleaved by **39**-Cu_3. This is not due to the inherently low reactivity of the substrate, nor to its insensitivity to copper(II) catalysis, as demonstrated by the finding that CpA is cleaved by [12]aneN_3-Cu and **38**-Cu_2 about three times more rapidly than UpU. The efficiency of **39**-Cu_3 in the cleavage of UpU is similar to that of **37**-Cu_2, and this supports the view that **39**-Cu_3 uses only two 1,2-vicinal metal centres in the catalysis, the third metal ion acting as a more or less innocent spectator.

The copper(II) complexes of triazacyclododecane decorated calix[4]arenes also show high phosphodiesterase activity in the cleavage of oligomeric ribonucleotides (ACCAUC, CGCUGA, AGGUUAA, CAGGCC, CCGGCA and ACUAUC) having a radioactive phosphate label in the 5′-terminal position (water, pH 7.4, 50°C; Equation (7)) (*34*). Rate constants for the cleavage of all of the scissile bonds of oligoribonucleotides are obtained in a detailed kinetic analysis. There is an undeniable tendency for the catalytic efficiency to increase with the number of metal units in the copper (II) complexes, revealing variable extents of cooperation between metal centres of trimetallic and bimetallic complexes. In a number of cases, the 1,2-vicinal complex **37**-Cu_2 is superior to its distal regioisomer **38**-Cu_2, in line with what observed in the reactions of HPNP and UpU, but in other cases the reverse holds. A similar situation holds for the relative efficiency of trinuclear versus dinuclear complexes, with an observed reactivity order strongly depending on oligoribonucleotide identity. In any event, whenever the trinuclear complex is the best cleaving agent in the lot, a clear-cut evidence of the operation of trimetallic catalysis is lacking, since the advantage due to the third metal ion hardly exceeds a factor of 2.

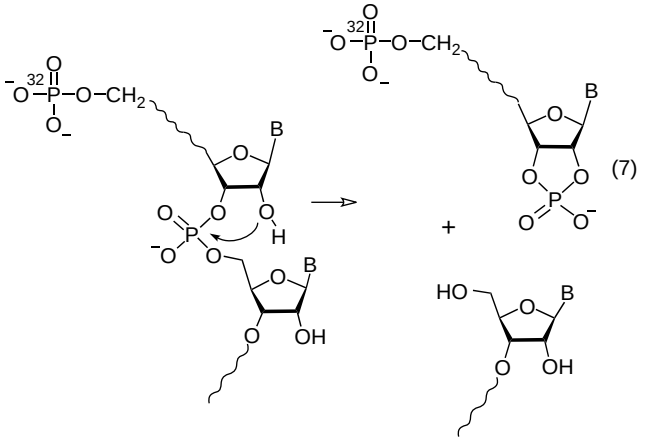

(7)

In marked contrast to the UpU and UpG selectivity observed in the reactions of diribonucleoside monophosphates, a remarkable preference for cleavage of the CpA bond of oligoribonucleotides is observed for all metal complexes. For example, the rate enhancement of *ca.* 5 $\times 10^5$-fold relative to background in the cleavage of the CpA bond in the hexamer CAGGCC by 50 μM **39**-Cu_3 is one of the highest values observed for the cleavage of ribonucleotides by synthetic metallonucleases. This picture is also confirmed in the reaction of the heptadecamer 5′-GCAAGCACAGACAUCAG-3′, in which all CpA bonds are cleaved by **37**-Cu_2, whereas other bonds do not react. A closely similar finding is obtained in the presence of **38**-Cu_2.

4. Calixarenes as chelators in olefin hydroformylation catalysts

Matt and co-workers (*35*) developed the series of rhodium complexes **40** provided with calixarene-based hemispherical chelators as effective and regioselective catalysts of olefin hydroformylation. In these chelate complexes, the metal centre is located in the tight molecular pocket defined by two symmetrically placed naphthyl moieties and by the two lateral pendent groups, anchored to 1,3-distal oxygen atoms of the macrocyclic skeleton. The conformational control is crucial. The large bite angle of the diphosphine ligand is associated with a *flattened-cone* conformation of the calix[4]arene, which results in a steeper orientation of the other pair of *O*-alkyl substituents towards the metal centre. As a consequence of the sterically hindered fit of reactants to the catalytic pocket, the hydroformylation of olefins catalysed by rhodium complexes **40** is highly regioselective, the formation of the linear aldehyde product being largely favoured over the branched counterpart (Equation (8)). In the hydroformylation of 1-octene with **40** (Z = propyl), a 58:1 linear to branched (*l*/*b*) aldehyde ratio is obtained. The *l*:*b* ratio significantly increased when the propyl groups were replaced by —CH_2Ph (*l*/*b* = 80) or by —CH_2naphthyl (no trace of the branched product is observed). In the hydroformylation of styrene, at variance with the output of the reaction carried out with conventional diphosphines, the linear aldehyde is obtained with selectivities as high as *ca.* 75% (**40**, Z = —CH_2Ph).

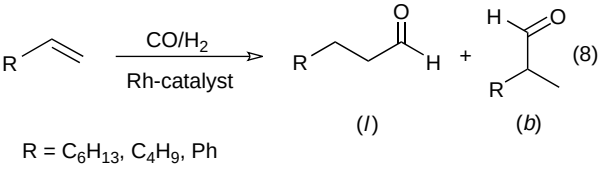

(8)

R = C_6H_{13}, C_4H_9, Ph

Neutral complexes **40** have been used in combination with calixarene-derived surfactants **41** in the aqueous hydroformylation of water-insoluble olefins (*36*). Good results in terms of turnover frequencies and of regioselectivity have been obtained in the hydroformylation of 1-octene, with linear to branched aldehyde ratios as high as 62.

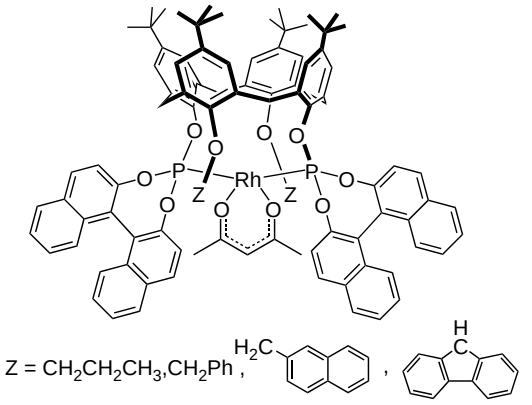

40

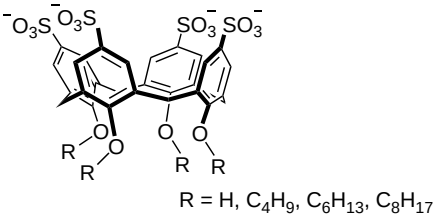

41

Water-soluble decasulphonated phosphacalix[4]arenes **42** were introduced by Shimizu et al. (*37*) as ligands for dual functional catalysis in the biphasic hydroformylation of water-insoluble olefins. Complexes **42**/[Rh(CO)$_2$(acac)] (acac = acetylacetonate) have been designed to act both as homogeneous metal catalysts and as inverse phase-transfer catalysts for transporting the organic substrate into the aqueous phase via inclusion in the hydrophobic cavity. Good levels of activity, stability and reusability have been obtained.

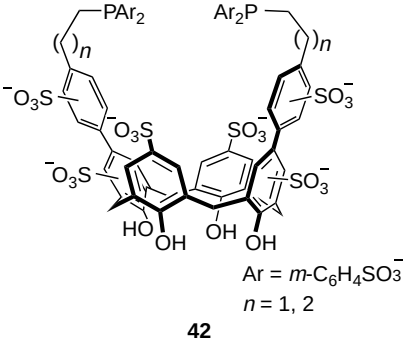

42

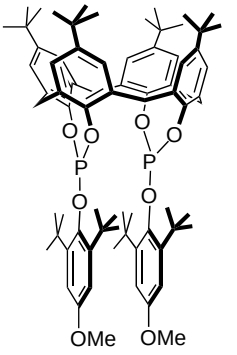

43

In the efficient Rh^{I} catalyst reported by Paciello et al. (*38*), the two phosphorous atoms of chelators are bonded to 1,2-vicinal oxygen atoms of the calix[4] arene platform. The hydroformylation of 1-octene with **43**/[Rh(CO)$_2$(acac)] proceeds slowly at 100°C and at low CO/H$_2$ pressure (20 bar), but a high selectivity in favour of the linear nonanal is observed, with $l/b = 200$.

Replacement of the two *tert*-butyl substituents in the aryloxy moieties of ligand **43** with isopropyl or methyl groups produced a controlled opening of the pincer-shaped structure of the ligand and gave more active and still highly regioselective catalysts ($l/b = 27$ and $l/b = 11$ with isopropyl and methyl groups, respectively).

5. Calixarenes as supramolecular protecting groups or supramolecular 'phlegmatisers'

A couple of examples are here mentioned in which, interestingly, the calixarene receptor acts as a sort of 'supramolecular protecting group' or 'phlegmatiser'. Formation of a supramolecular complex with substrate or reactant induces a selective transformation otherwise difficult to achieve.

Reinaud and co-workers (*39*) described the remarkably regioselective mono-carbamoylation of the unsymmetrical triamine *N*-(2-aminoethyl)propane-1,3-diamine (**44**).

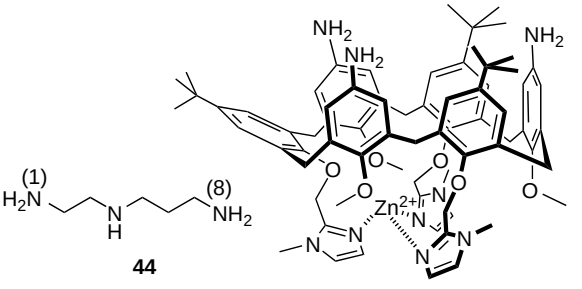

44

45-Zn

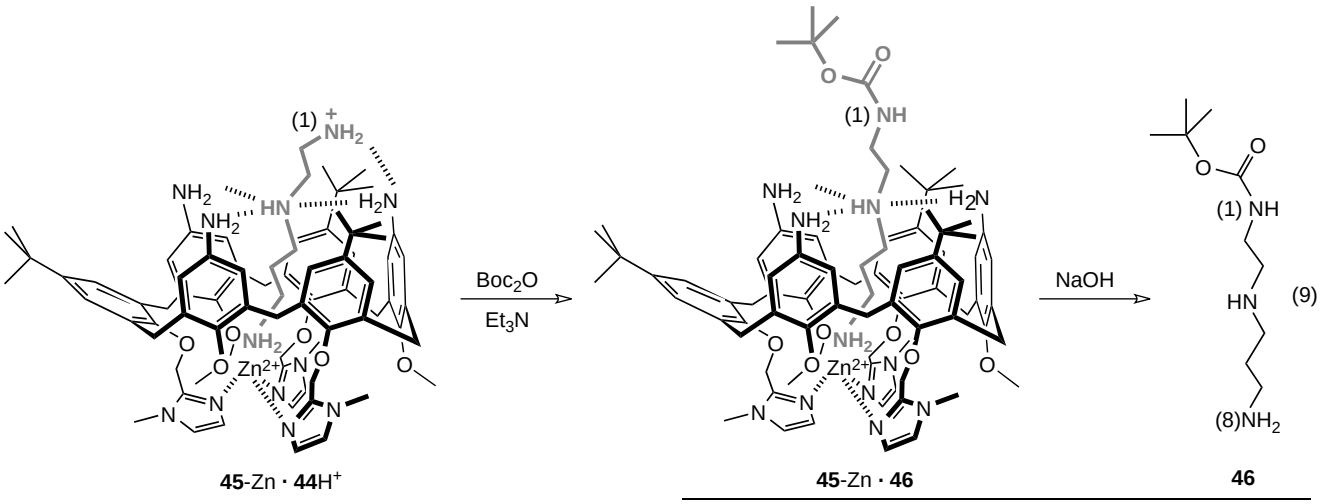

Metallocalixarene **45**-Zn acts as a multipoint recognition host for polyfunctionalised guests. The calix[6]arene platform, decorated with three imidazole arms at the lower rim, is conveniently preorganised in *cone* conformation upon binding to zinc(II) ions. The three imidazole arms wrap the metal ion, leaving a single coordination site accessible for guest binding inside a funnel-like cavity, which is 'shaped' by zinc(II) ion complexation. The oxygen atoms at the lower rim and the NH_2 substituents at the upper rim may participate in multitopic recognition processes via H-bonding. As a result of multiple interactions, the unsymmetrical triamine guest **44** is complexed to **45**-Zn and oriented with high regioselectivity, so that the calixarene cavity surrounds two amino groups out of three, and the electrophilic reagent (Boc_2O) reacts at a single site (N1) with an unprecedented chemo- and regioselectivity (Equation 9). The regioselectively monoprotected derivative N1-monocarbamate **46**, isolated for the first time, is obtained in high yield on a preparative scale. Thus, a sort of supramolecular protection of a multifunctional substrate is achieved and a transformation which would be impracticable with conventional covalent chemistry is obtained.

The limited size of the calix[4]arene cavity allows deep penetration of only small guests. Highly stable 1:1 complex ($K > 5 \times 10^8\,M^{-1}$) showing no sign of decomposition for several months, both in solution and in the solid state, is formed between tetra-*O*-methylated *p*-*tert*-butylcalix[4]arene and nitrosonium ion NO^+ in CH_2Cl_2 (*40*).

Rudkevich and co-workers (*41*) discovered that caged NO^+ complexes are formed on bubbling NO_2/N_2O_4 through a chloroform solution of tetra-*O*-alkylated calix[4]arene (**47**, R = hexyl) fixed in the 1,3-*alternate* conformation, in the presence of $SnCl_4$ (Equation (10)). Chemical properties of encapsulated

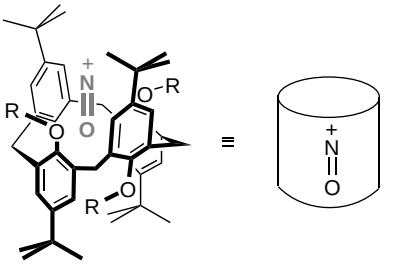

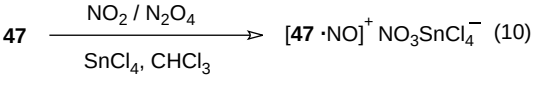

NO^+ are different from those in free solution. Nitrosonium ion, safely entrapped in the cavity of **47**, acts as a highly selective nitrosating agent towards secondary amides (Scheme 4). Calix[4]arene **47** may then be considered as a useful dispenser of a nitrosating agent of peculiar selectivity. Size-shape selectivity is observed, the reactivity of encapsulated NO^+ being controlled by the calix[4]arene cavity. The reaction is quite sensitive to the size of the alkyl group (*Alk*), but not to that of *Alk′*. Fair to good yields (50–95%) of *N*-nitrosated products are obtained with *N*-methylated amides, independent of the size of *Alk′*, from ethyl to heptyl. No reaction occurs with amides

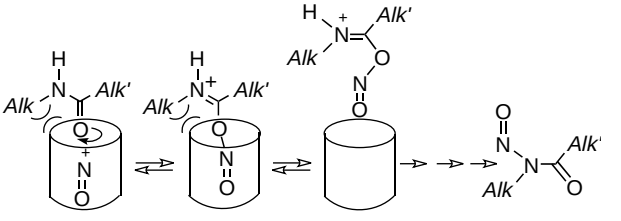

Scheme 4. Proposed mechanism of *N*-nitrosation of secondary amides with encapsulated **47**-NO^+.

alkylated with *Alk* bulkier than methyl, on account of the hindered approach to the encapsulated NO^+ reactant.

6. Carbonyl and phosphoryl groups organised on the calixarene scaffold: special reactivity features

Calixarenes have not only proved to be versatile platforms in the fabrication of mono- and multitopic ligands for molecular recognition or supramolecular catalysis, but also strategical 'meeting points' of functional groups, which can show special or unique reactivity features thanks to their preorganised arrangement at the lower or upper rim. A case in point is the reactivity pattern observed with formylated *cone*-calix[4]arenes **48**–**51**. The 1,3-distal diformylated *cone*-calix[4]arene **48** undergoes intramolecular Cannizzaro disproportionation in the presence of a strong base (Scheme 5), thus providing an easy route to desymmetrisation of 1,3-distal diformylated calix[4]arenes, while its 1,2-vicinal regioisomer **49** and the analogous monoaldehyde **50** are unreactive under the same conditions (*42*).

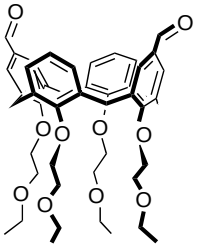

48

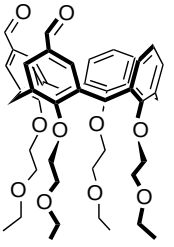

49

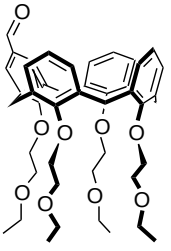

50

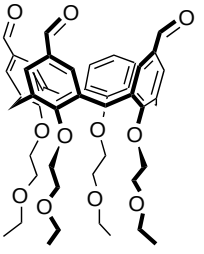

51

The close proximity of the two 1,3-distal functional groups

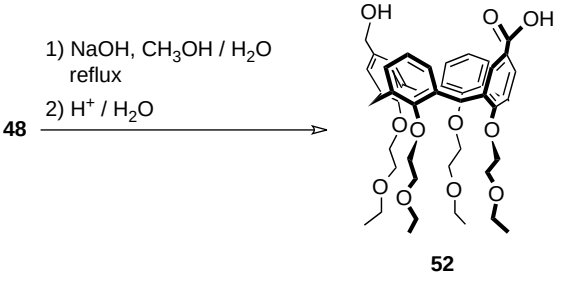

Scheme 5. Intramolecular Cannizzaro disproportionation of dialdehyde **48**.

in the *flattened-cone* conformation of **48** effectively promotes the intramolecular hydride transfer from the anionic tetrahedral intermediate at one reaction centre to the 1,3-distal formyl carbonyl (**IV**). The geometrical arrangement of the two reacting groups in the 1,2-vicinal regioisomer **49** does not allow, on the other hand, an analogous intramolecular transfer of hydride via a reasonably unstrained transition state, and no disproportionation occurs under the reaction conditions (3 days of refluxing in 0.2 M NaOH, 70% aqueous methanol).

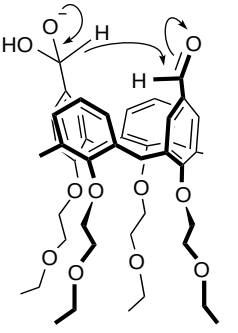

IV

The high intramolecular reactivity of the 1,3-distal regioisomer **48** was quantified in terms of EM. The Cannizzaro reaction of *p*-methoxybenzaldehyde was taken as a suitable intermolecular model counterpart and pertinent rate data were extrapolated from data reported in the literature for this much slower process (*43*). An EM value as high as 6×10^2 M indicates high efficiency of hydride transfer from the anionic tetrahedral function to the neighbouring carbonyl group, and compares well with the EM values of highly efficient nucleophilic additions to carbonyl groups involving the formation of 5- and 6-membered rings from conformationally mobile reactants (*11b*).

The highly selective 1,3-distal intramolecular Cannizzaro disproportionation was put to the useful purpose of a convenient one-step preparation of the inherently chiral (*44*) trifunctional derivative **53** from the easily available (*27*) *cone*-triformylcalix[4]arene **51** (*45*). Only the two formyl groups in the 1,3-distal arrangement react to give the Cannizzaro reaction under the adopted conditions (0.010 M **51** in 70% aqueous methanol, 3 days reflux in the presence of 0.20 M NaOH), with the third formyl group acting as an innocent spectator (Scheme 6). At variance with the symmetrical reagent **51**, the ABCH-substituted *cone*-calix[4]arene product **53** of the disproportionation process is inherently chiral, as a consequence of an asymmetric substitution pattern in a non-planar molecular framework, and a racemic mixture of the two enantiomers (*cR*)-**53** and (*cS*)-**53** (*46*) was obtained (Scheme 6).

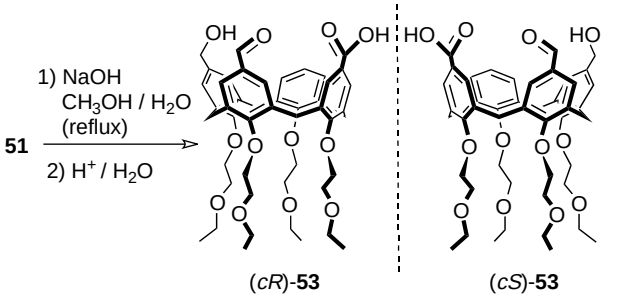

Scheme 6. Intramolecular Cannizzaro disproportionation of trialdehyde **51**.

The presence of three different functional groups (—CH_2OH, —CHO and —COOH) at the upper rim of the calixarene scaffold makes **53** a promising and versatile intermediate for the development of multifunctional devices, with possible applications in multifunctional or/and asymmetric catalysis or in the specific recognition of multifunctional biological substrates. Interesting chiral discrimination with a 39% diastereomeric excess was observed (*45*) in the reversible imine formation (*47*) with equimolar (5.0 mM) L-serine ethyl ester hydrochloride in the presence of excess solid K_2CO_3 (acetonitrile, 25°C). The observed enantioselectivity was ascribed to a multipoint-interaction involving hydrogen bonding of the hydroxyl group of the amino acid side chain with the upper rim functional groups. Consistently, chiral discrimination was not observed with alanine and valine derivatives, lacking hydrogen bonding groups on the side chain.

An interesting example of intramolecular rearrangement at calixarenes, involving in this case functional groups at lower rim, was reported by Markovski et al. (*48*). In a one-pot procedure, monosodium derivatives of *cone*-1,3-*bis*(diethoxyphosphoryl)-calix[4]arenes **54** undergo *O*,*O*-phosphorotropic rearrangement into the sodium salt **57** of 1,2-*bis*(diethoxyphosphoryl)calix[4]arenes, which upon treatment with electrophilic reagents such as benzoyl chloride or methyl monobromoacetate are converted into the racemic mixture of calix[4]arenes **58** with asymmetric AABH substitution at the lower rim (Scheme 7). The key step of this process is the *O*,*O*-phosphorotropic rearrangement via the highly favoured intramolecular attack of the phenolate nucleophile at the 1,2-vicinal phosphorus atom giving the short-lived phosphorane intermediate **56**.

7. Conclusions

In this overview, focussing on processes controlled by calixarenes and involving carbonyl and phosphoryl groups, we have shown examples of high levels of cooperation among recognition and catalytic sites conveniently preorganised on a calixarene platform. Special reactivity features induced by proximity of phosphoryl or carbonyl functional groups at the upper or lower rim of calixarenes have been also described.

Dynamic preorganisation on the calixarene scaffold of two or more structural units that can serve as recognition and/or catalytic sites is highly convenient in the design of efficient supramolecular catalysts. A residual flexibility is crucial in the dynamic fit of the catalyst to the bound substrate in its transformation into the transition state, and prevents severe risks of failure connected to the design of

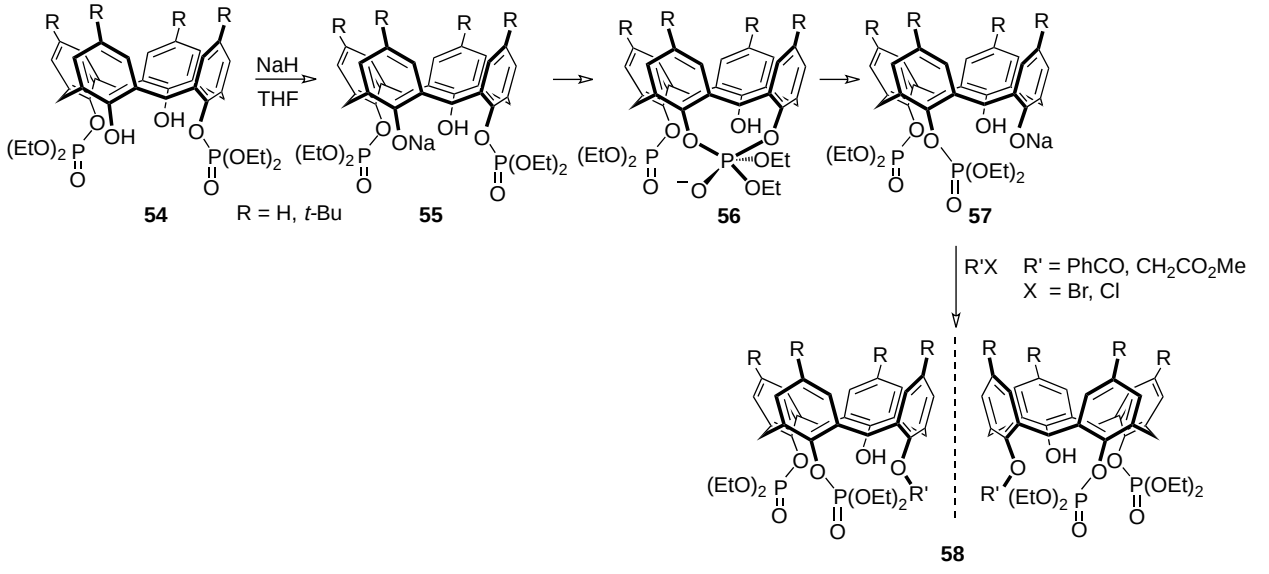

Scheme 7. *O*,*O*-phosphorotropic rearrangement of 1,3-*bis*(diethoxyphosphoryl)calix[4]arenes **54**.

tailored, perfectly 'fitting' and rigid receptors for the selective recognition of the transition state.

An ideal target of future investigations might be the introduction on the calixarene framework of interchangeable recognition and catalytic units via reversible connections, thus making the molecular platform of calixarenes a recoverable and versatile scaffold for the fabrication of a multi-purpose 'lab on a macrocycle'.

References

(1) (a) Gutsche, C.D. *Calixarenes*; The Royal Society of Chemistry: Cambridge, 1989; (b) Gutsche, C.D. *Calixarenes Revisited*; The Royal Society of Chemistry: Cambridge, 1998; (c) Vicens, J., Böhmer, V., Eds.; *Calixarenes: A Versatile Class of Macrocyclic Compounds*; Kluwer: Dordrecht, 1991; (d) Mandolini, L., Ungaro, R., Eds.; *Calixarenes in Action*; Imperial College Press: London, 2000; (e) Asfari, Z., Böhmer, V., Harrowfield, J., Vicens, J., Eds.; *Calixarenes*; Kluwer: Dordrecht, 2001; (f) Vicens, J., Harrowfield, J., Eds.; *Calixarenes in the Nanoworld*; Springer: Dordrecht, 2006; (g) Cacciapaglia, R.; Di Stefano, S.; Mandolini, L. In *Molecular Encapsulation: Organic Reactions in Constrained Systems*: Brinker, U.H., Mieusset, J.-L., Eds.; Wiley: New York, 2010, Chapter 8, pp 201–225.

(2) (a) Casnati, A.; Sansone, F.; Ungaro, R. *Acc. Chem. Res.* **2003**, *36*, 246–254; (b) Matthews, S.E.; Beer, P.D. *Supramol. Chem.* **2005**, *17*, 411–435; (c) Baldini, L.; Casnati, A.; Sansone, F.; Ungaro, R. *Chem. Soc. Rev.* **2007**, *36*, 254–266; (d) Kim, J.S.; Quang, D.T. *Chem. Rev.* **2007**, *107*, 3780–3799; (e) Biros, S.M.; Rebek, J. Jr. *Chem. Soc. Rev.* **2007**, *36*, 93–104; (f) Maes, W.; Dehaen, W. *Chem. Soc. Rev.* **2008**, *37*, 2393–2402; (g) Coleman, A.W.; Jebors, S.; Shahgaldian, P.; Ananchenko, G.S.; Ripmeester, J.A. *Chem. Commun.* **2008**, 2291–2303; (h) Homden, D.M.; Redshaw, C. *Chem. Rev.* **2008**, *108*, 5086–5130; (i) Sansone, F.; Baldini, L.; Casnati, A.; Ungaro, R. *New J. Chem.* **2010**, *34*, 2715–2728; (j) Sansone, F.; Casnati, A. *Chem. Soc. Rev.* **2013**, *42*, 4623–4739; (k) Casnati, A. *Chem. Commun.* **2013**, *49*, 6827–6830.

(3) Molenveld, P.; Engbersen, J.F.J.; Reinhoudt, D.N. *Chem. Soc. Rev.* **2000**, *29*, 75–86.

(4) Cacciapaglia, R.; Casnati, A.; Mandolini, L.; Ungaro, R. *J. Am. Chem. Soc.* **1992**, *114*, 10956–10958.

(5) (a) Cacciapaglia, R.; Casnati, A.; Mandolini, L.; Ungaro, R. *Chem. Commun.* **1992**, 1291–1293; (b) Cacciapaglia, R.; van Doorn, A.R.; Mandolini, L.; Reinhoudt, D.N.; Verboom, W. *J. Am. Chem. Soc.* **1992**, *114*, 2611–2617. (c) Cacciapaglia, R.; Mandolini, L. *Chem. Soc. Rev.* **1993**, *22*, 221–231.

(6) Kraft, D.; Böhmer, V.; Cacciapaglia, R.; Mandolini, L.; Vogt, W.; **1999**, Unpublished results.

(7) Baldini, L.; Bracchini, C.; Cacciapaglia, R.; Casnati, A.; Mandolini, L.; Ungaro, R. *Chem. Eur. J.* **2000**, *6*, 1322–1330.

(8) See, for example: (a) Weston, J. *Chem. Rev.* **2005**, *105*, 2151–2174; (b) Cowan, J.A. *Chem. Rev.* 1998, **98**, 1067–1087; (c) Wilcox, D.E. *Chem. Rev.* **1996**, *96*, 2435–2458.

(9) (a) Gruber, B.; Kataev, E.; Aschenbrenner, J.; Stadlbauer, S.; König, B. *J. Am. Chem. Soc.* **2011**, *133*, 20704–20707; (b) Panja, A.; Matsuo, T.; Nagao, S.; Hirota, S. *Inorg. Chem.* **2011**, *50*, 11437–11445; (c) Linjalahti, H.; Feng, G.Q.; Mareque-Rivas, J.C.; Mikkola, S.; Williams, N.H. *J. Am. Chem. Soc.* **2008**, *130*, 4232–4233; (d) Nwe, K.; Andolina, C.M.; Morrow, J.R. *J. Am. Chem. Soc.* **2008**, *130*, 14861–14871; (e) Wang, Q.; Lönnberg, H. *J. Am. Chem. Soc.* **2006**, *128*, 10716–10728; (f) O'Donoghue, A.; Pyun, S.Y.; Yang, M.Y.; Morrow, J.R.; Richard, J.P. *J. Am. Chem. Soc.* **2006**, *128*, 1615–1621; (g) Neverov, A.A.; Lu, Z.-L.; Maxwell, C. I.; Mohamed, M.F.; White, C.J.; Tsang, J.S.W.; Brown, R.S. *J. Am. Chem. Soc.* **2006**, *128*, 16398–16405.

(10) Cacciapaglia, R.; Casnati, A.; Di Stefano, S.; Mandolini, L.; Paolemili, D.; Reinhoudt, D.N.; Sartori, A.; Ungaro, R. *Chem Eur. J.* **2004**, *10*, 4436–4442.

(11) (a) Kirby, A.J. *Adv. Phys. Org. Chem.* **1980**, *17*, 183–278; (b) Mandolini, L. *Adv. Phys. Org. Chem.* **1986**, *22*, 1–111.

(12) Cacciapaglia, R.; Di Stefano, S.; Mandolini, L. *Acc. Chem. Res.* **2004**, *37*, 113–122.

(13) Cacciapaglia, R.; Di Stefano, S.; Kelderman, E.; Mandolini, L. *Angew. Chem. Int. Ed.* **1999**, *38*, 348–351.

(14) Cacciapaglia, R.; Casnati, A.; Mandolini, L.; Reinhoudt, D. N.; Salvio, R.; Sartori, A.; Ungaro, R. *J. Org. Chem.* **2005**, *70*, 624–630.

(15) Cacciapaglia, R.; Casnati, A.; Mandolini, L.; Reinhoudt, D. N.; Salvio, R.; Sartori, A.; Ungaro, R. *J. Org. Chem.* **2005**, *70*, 5398–5402.

(16) Cacciapaglia, R.; Casnati, A.; Mandolini, L.; Reinhoudt, D. N.; Salvio, R.; Sartori, A.; Ungaro, R. *Inorg. Chim. Acta* **2007**, *360*, 981–986.

(17) Hioki, H.; Nishimoto, R.; Kawaguchi, K.; Kubo, M.; Harada, K.; Fukuyama, Y. *Chem. Commun.* **2009**, 7194–7196.

(18) Shinkai, S.; Mori, S.; Koreishi, H.; Tsubaki, T.; Manabe, O. *J. Am. Chem. Soc.* **1986**, *108*, 2409–2416.

(19) Goto, K.; Yano, Y.; Okada, E.; Liu, C.-W.; Yamamoto, K.; Ueoka, R. *J. Org. Chem.* **2003**, *68*, 865–870.

(20) (a) Magrans, J.O.; Ortiz, A.R.; Molins, A.; Lebouille, P.H. P.; Sánchez-Quesada, J.; Prados, P.; Pons, M.; de Mendoza, J. *Angew. Chem. Int. Ed.* **1996**, *35*, 1712–1715; (b) Cuevas, F.; Di Stefano, S.; Magrans, J.O.; Prados, P.; Mandolini, L.; de Mendoza, J. *Chem. Eur. J.* **2000**, *6*, 3228–3234.

(21) Cotton, F.A.; Hazen, Jr, E.E.; Legg, M.J. *Proc. Natl. Acad. Sci. U.S.A.* **1979**, *76*, 2551–2555.

(22) (a) Suh, J.; Moon, S.-J. *Inorg. Chem.* **2001**, *40*, 4890–4895; (b) Ait-Haddou, H.; Sumaoka, J.; Wiskur, S.L.; Folmer-Andersen, J.F.; Anslyn, E.V. *Angew. Chem. Int. Ed.* **2002**, *41*, 4014–4016; (c) Piatek, A.M.; Gray, M.; Anslyn, E.V. *J. Am. Chem. Soc.* **2004**, *126*, 9878–9879; (d) Scheffer, U.; Strick, A.; Ludwig, V.; Peter, S.; Kalden, E.; Göbel, M.W. *J. Am. Chem. Soc.* **2005**, *127*, 2211–2217; (e) Gnaccarini, C.; Peter, S.; Scheffer, U.; Vonhoff, S.; Klussmann, S.; Göbel, M.W. *J. Am. Chem. Soc.* **2006**, *128*, 8063–8067; (f) Lindgren, N.J.V.; Lars Geiger, J.R.; Schmuck, C.; Baltzer, L. *Angew. Chem., Int. Ed.* **2009**, *48*, 6722–6725; (g) Corona-Martinez, D.O.; Taran, O.; Yatsimirsky, A.K. *Org. Biomol. Chem.* **2010**, *8*, 873–880; (h) Salvio, R.; Cacciapaglia, R.; Mandolini, L. *J. Org. Chem.* **2011**, *76*, 5438–5443; (i) Salvio, R.; Mandolini, L.; Savelli, C. *J. Org. Chem.* **2013**, *78*, 7259–7263.

(23) Baldini, L.; Cacciapaglia, R.; Casnati, A.; Mandolini, L.; Salvio, R.; Sansone, F.; Ungaro, R. *J. Org. Chem.* **2012**, *77*, 3381–3389.

(24) Salvio, R.; Casnati, A.; Mandolini, L.; Sansone, F.; Ungaro, R. *Org. Biomol. Chem.* **2012**, *10*, 8941–8943.

(25) (a) Hosseini, M.W.; Lehn, J.-M.; Jones, K.C.; Plute, K.E.; Mertes, K.B.; Mertes, M.P. *J. Am. Chem. Soc.* **1989**, *111*, 6330–6335; (b) Hosseini, M.W.; Lehn, J.-M.; Maggiora, L.;

Mertes, K.B.; Mertes, M.P. *J. Am. Chem. Soc.* **1987**, *109*, 537–544; (c) Hosseini, M.W.; Lehn, J.-M.; Mertes, M.P. *Helv. Chim. Acta* **1983**, *66*, 2454–2466.
(26) Molenveld, P.; Kapsabelis, S.; Engbersen, J.F.J.; Reinhoudt, D.N. *J. Am. Chem. Soc.* **1997**, *119*, 2948–2949.
(27) Molenveld, P.; Stikvoort, W.M.G.; Kooijman, H.; Spek, A. L.; Engbersen, J.F.J.; Reinhoudt, D.N. *J. Org. Chem.* **1999**, *64*, 3896–3906.
(28) Molenveld, P.; Engbersen, J.F.J.; Kooijman, H.; Spek, A.L.; Reinhoudt, D.N. *J. Am. Chem. Soc.* **1998**, *120*, 6726–6737.
(29) Sträter, N.; Lipscomb, W.N.; Klabunde, T.; Krebs, B. *Angew. Chem. Int. Ed.* **1996**, *35*, 2024–2055.
(30) Molenveld, P.; Engbersen, J.F.J.; Reinhoudt, D.N. *Angew. Chem. Int. Ed.* **1999**, *38*, 3189–3192.
(31) Cacciapaglia, R.; Casnati, A.; Mandolini, L.; Reinhoudt, D. N.; Salvio, R.; Sartori, A.; Ungaro, R. *J. Am. Chem. Soc.* **2006**, *128*, 12322–12330.
(32) Kimura, E.; Shiota, T.; Koike, T.; Shiro, M.; Kodama, M. *J. Am. Chem. Soc.* **1990**, *112*, 5805–5811.
(33) Zompa, L. *Inorg. Chem.* **1978**, *17*, 2531–2536.
(34) Cacciapaglia, R.; Casnati, A.; Mandolini, L.; Peracchi, A.; Reinhoudt, D.N.; Salvio, R.; Sartori, A.; Ungaro, R. *J. Am. Chem. Soc.* **2007**, *129*, 12512–12520.
(35) (a) Sémeril, D.; Jeunesse, C., Matt, D., Toupet, L. *Angew. Chem. Int. Ed.* **2006**, *45*, 5810–5814; (b) Sémeril, D.; Matt, D., Toupet, L. *Chem. Eur. J.* **2008**, *14*, 7144–7155; and references therein.
(36) Monnereau, L.; Sémeril, D.; Matt, D.; Toupet, L. *Adv. Synth. Catal.* **2009**, *351*, 1629–1636.
(37) Shimizu, S.; Shirakawa, S.; Sasaki, Y.; Hirai, C. *Angew. Chem. Int. Ed.* **2000**, *39*, 1256–1259.
(38) Paciello, R.; Siggel, L.; Röper, M. *Angew. Chem. Int. Ed.* **1999**, *38*, 1920–1923.
(39) Coquière, D.; de la Lande, A.; Parisel, O.; Prangé, T.; Reinaud, O. *Chem. Eur. J.* **2009**, *15*, 11912–11917.
(40) Rathore, R.; Lindeman, S.V.; Rao, K.S.S.P.; Sun, D.; Kochi, J.K. *Angew. Chem. Int. Ed.* **2000**, *39*, 2123–2127.
(41) (a) Zyryanov, G.V.; Kang, Y.; Rudkevich, D.M. *J. Am. Chem. Soc.* **2003**, *125*, 2997–3007; (b) Kang, Y.; Zyryanov, G.V.; Rudkevich, D. *Chem. Eur. J.* **2005**, *11*, 1924–1932.
(42) Galli, M.; Berrocal, J.A.; Di Stefano, S.; Cacciapaglia, R.; Mandolini, L.; Baldini, L.; Casnati, A.; Ugozzoli, F. *Org. Biomol. Chem.* **2012**, *10*, 5109–5112.
(43) Tommila, E. *Ann. Acad. Sci. Fennicae* **1942**, *A59* (8), 3–69.
(44) (a) Zheng, Y.-S.; Luo, J. *J. Incl. Phenom. Macrocycl. Chem.* **2011**, *71*, 35–56; (b) McIldowie, M.J.; Mocerino, M.; Ogden, M.I. *Supramol. Chem.* **2010**, *22*, 13–39, and references therein.
(45) Ciaccia, M.; Tosi, I.; Cacciapaglia, R.; Casnati, A.; Baldini, L.; Di Stefano, S. *Org. Biomol. Chem.* **2013**, *11*, 3642–3648.
(46) Dalla Cort, A.; Mandolini, L.; Pasquini, C.; Schiaffino, L. *New J. Chem.* **2004**, *28*, 1198–1199.
(47) Ciaccia, M.; Cacciapaglia, R.; Mencarelli, P.; Mandolini, L.; Di Stefano, S. *Chem. Sci.* **2013**, *4*, 2253–2261.
(48) Markovsky, L.N.; Visotsky, M.A.; Pirozhenko, V.V.; Kalchenko, V.I.; Lipkowski, J.; Simonov, Y.A. *Chem. Commun.* **1996**, 69–71.